Published in final edited form as:
J Am Coll Cardiol. 2010 April 13; 55(15): 1629–1638. doi:10.1016/j.jacc.2009.08.089.

Impaired infarct healing in atherosclerotic mice with Ly-6C^{hi} monocytosis

Peter Panizzi, PhD[1,2], **Filip K. Swirski, PhD**[1,2], **Jose-Luiz Figueiredo, MD**[1,2], **Peter Waterman, BS**[1,2], **David E. Sosnovik, MD**[2,3], **Elena Aikawa, MD, PhD**[2], **Peter Libby, MD**[4], **Mikael Pittet, PhD**[1], **Ralph Weissleder, MD, PhD**[1,2], and **Matthias Nahrendorf, MD, PhD**[1,2]

[1]Center for Systems Biology, Massachusetts General Hospital and Harvard Medical School, Simches Research Building, 185 Cambridge St., Boston, MA 02114

[2]Center for Molecular Imaging Research, Massachusetts General Hospital and Harvard Medical School, Building 149, 13th St., Charlestown, MA 02129

[3]Cardiology Division, Massachusetts General Hospital and Harvard Medical School

[4]Cardiovascular Division, Department of Medicine, Brigham & Women's Hospital, 75 Francis Street, Boston, MA 02115

Abstract

Objective—To test if blood monocytosis in mice with atherosclerosis affects infarct healing.

Background—Monocytes are cellular protagonists of tissue repair and their specific subtypes regulate the healing program after MI. Inflammatory Ly-6C^{hi} monocytes dominate on day 1-4 and digest damaged tissue; reparative Ly-6C^{lo} monocytes dominate on day 5-10 and promote angiogenesis and scar formation. However, the monocyte repertoire is disturbed in atherosclerotic mice: Ly-6C^{hi} monocytes expand selectively, which may disrupt the resolution of inflammation.

Methods and Results—Ex vivo analysis of 5 day-old infarcts showed >10-times more Ly-6C^{hi} monocytes in atherosclerotic (apoE$^{-/-}$) mice compared to wild type mice. The injured tissue in apoE$^{-/-}$ mice also showed a more pronounced inflammatory gene expression profile (e.g. increased TNF-α and MPO and decreased TGF-β) and a higher abundance of proteases, which are associated with the activity of Ly-6C^{hi} monocytes. To relate inflammatory activity to left ventricular remodeling, we used a combination of noninvasive molecular and physiologic imaging. FMT-CT on day 5 post MI showed higher proteolysis and phagocytosis in infarcts of atherosclerotic mice. Serial MRI showed accelerated deterioration of EF between day 1 and 21 after MI in apoE$^{-/-}$. Finally, we could recapitulate these features in wild-type mice with artificially–induced Ly-6C^{hi} monocytosis.

Conclusion—Ly-6C^{hi} monocytosis disturbs resolution of inflammation in murine infarcts and consequently enhances left ventricular remodeling. These findings position monocyte subsets as potential therapeutic targets to augment tissue repair after infarction and to prevent post-MI heart failure.

Corresponding author: Ralph Weissleder or Matthias Nahrendorf, Center for Systems Biology, 185 Cambridge Street, Boston, MA 02114, Tel: (617) 643-0500, Fax: (617) 643-6133, rweissleder@mgh.harvard.edu, mnahrendorf@mgh.harvard.edu.

Conflict of Interest Disclosures: Ralph Weissleder and Peter Waterman own shares of VisEn Medical.

Introduction

In the first week after coronary occlusion, the myocardium experiences high cell and extracellular matrix turnover[1-4] and is exposed to the constant stress of cycling intra-cardiac pressures. The quality of infarct healing determines the mechanical properties of the injured tissue and therefore prognosis: poor healing may lead to infarct rupture or left ventricular dilation due to infarct expansion.5 Timely reperfusion therapy reduces acute infarct mortality,6 and current standard of care attenuates post MI remodeling.[7, 8] However, present therapies typically have modest long-term effects: for example, the Survival and Ventricular Enlargement (SAVE) trial indicated that angiotensin-converting enzyme (ACE) inhibitors can only reduce infarct mortality from 25 to 20%;[9] and mortality remains even higher in patients with end-stage heart failure.10 Thus, there is a need to understand better the complex cellular and molecular constituents that regulate myocardial healing and remodeling as they may serve as biomarkers and therapeutic targets for the prediction and prevention of heart failure.

Recruitment of monocytes from the bloodstream into the vessel wall drives atherosclerotic plaque growth and vulnerability.[11] Blood levels of inflammatory Ly-6C^{hi} monocytes increase profoundly in atherosclerotic mice,[12, 13] and peripheral monocytosis occurs in patients with coronary artery disease.[14, 15] At the same time, Ly-6C^{hi} monocytes dominate in the myocardial wound on day 1-4 after coronary ligation and digest necrotic tissue (monocytic Phase 1).[16] During a second monocytic phase that ensues directly (Phase 2), the number of Ly-6C^{hi} monocytes declines rapidly while reparative Ly-6C^{lo} monocytes accumulate and propagate healing and the resolution of inflammation. Abrogation of either monocytic phase results in poor healing, indicating that successful cardiac wound repair depends on a well-coordinated bi-phasic monocyte response.[16] The present study tested the hypothesis that atherosclerosis-associated Ly-6C^{hi} blood monocytosis interferes with resolution of inflammation during the monocytic Phase 2 of infarct healing. Based on clinical data showing that blood monocytosis independently associates with heart failure after MI,[17, 18] we hypothesized that pre-existing blood monocytosis in atherosclerotic mice increases and prolongs the presence of Ly-6C^{hi} monocytes in the infarct, interferes with resolution of inflammation after ischemic injury, enhances left ventricular remodeling and thus ultimately favors heart failure. This hypothesis has considerable clinical relevance because inflammation predisposes to complications of atherosclerosis such as acute myocardial infarction.[11]

While inflammation is typically assessed with ex vivo techniques, non-invasive tools that gauge inflammation can be used to relate innate immune cell function in the infarct with ventricular dilation and subsequent development of heart failure. Here we used Fluorescence Molecular Tomography in conjunction with anatomical Computed Tomography (FMT-CT) and MRI for in vivo assessment of cellular responses and physiological consequences otherwise hard to measure longitudinally.

Materials and Methods

Mouse model

C57B/6 and apoE$^{-/-}$ mice were purchased from Jackson Labs. ApoE$^{-/-}$ mice had an average age of 45 weeks and were on a high-cholesterol diet (Harlan Teklad, 0.2% total cholesterol). MI was induced by coronary ligation as described before.19 We first conducted an invasive study that assessed monocyte numbers and the quality of inflammation and healing by flow cytometric and molecular profiling of infarcts harvested on day 5 after MI. We next investigated the interrelation of infarct healing and ventricular dilation in a longitudinal trial with serial MRI on day 1 and 21 and FMT-CT imaging on day 5 after MI. To study the

impact of blood monocytosis on infarct healing in a model independent of lipid metabolism, we induced blood monocytosis in C57B/6 mice (50μg of lipopolysaccharide (Sigma) i.p. injections20 24 hours prior to and on days 1, 2, 3, and 4 after MI). The contribution of neutrophils to healing in apoE$^{-/-}$ mice was assessed in a cohort in which we depleted neutrophils (500 mg i.p. injections of anti Ly-6G antibody (BioXCell) 24 hours prior to and on day 1 and 3 after MI). The experimental protocol and animal numbers are outlined in Figure 1. The local institutional animal welfare committee approved the research reported.

Flow cytometry

On day 5 after MI, peripheral blood and infarct tissue was prepared for flow cytometric quantitation of leukocytes as described before.[16] Cell suspensions were incubated with a cocktail of mAbs against T cells (CD90-PE, 53-2.1), B cells (B220-PE, RA3-6B2), NK cells (CD49b-PE, DX5 and NK1.1-PE, PK136), granulocytes (Ly-6G-PE, 1A8), myeloid cells (CD11b-APC, M1/70), antigen-presenting cells (I-A^b (AF6-120.1)-biotin-Strep-PerCP) and monocyte subsets (Ly-6C-FITC, AL-21) (BD Biosciences). Monocytes were identified as CD11b^{hi} (CD90/B220/CD49b/NK1.1/Ly-6G)^{lo} (F4/80/I-A^b/CD11c)^{lo} Ly-6C$^{hi/lo}$. Macrophages/dendritic cells were identified as CD11b^{hi} (CD90/B220/CD49b/NK1.1/Ly-6G)^{lo} (I-A^b/CD11c)^{hi} Ly-6C^{lo}. Neutrophils were identified as CD11b^{hi} (CD90/B220/CD49b/NK1.1/Ly-6G)^{hi} (I-A^b/CD11c)^{lo} Ly-6C^{int}. Monocyte and macrophage cell numbers were calculated as total cells multiplied by percent cells within the monocyte/macrophage gate. Within this population, monocyte subsets were identified as (I-A^b/CD11c)^{lo} and either Ly-6C^{hi} or Ly-6C^{lo}. For assessment of proteolytic activity including cathepsins 5 nmol Prosense-680 (VisEn Medical) was injected into the tail vein 24h prior to sacrifice. For assessment of phagocytic activity, CLIO-VT750 (CMIR Chemistry Core), 15mg of Fe /kg bodyweight,[21] was injected into the tail vein 24 h prior to sacrifice. Data were acquired on an LSRII (BD Biosciences).

Pathology

Immunoreactive staining—Serial 6 μm thick sections were stained for neovessels (CD31, BD Pharmingen), VEGF (Abcam), proteases (cathepsin B, Santa Cruz Biotechnology and matrix metalloproteinase (MMP) 2 and 9, Millipore), and macrophages (F4/80, Abcam). We quantified the percentage positive area within the field of view using 5 high power fields (magnification ×200) per section and per animal.

Fluorescence reflectance imaging—On day 5 post MI, short axis rings were imaged at 4× magnification (OV-110, Olympus, Center Valley, PA) in the 680 and 750 nm channels 24 hours after injection of Prosense-680 and CLIO-750.

Quantitative PCR—Multiplex quantitative PCR was performed on triplicate samples using Applied Biosystems TaqMan® Assays. Infarct tissue was examined for expression of markers of inflammatory monocytes (Ly-6C, Mm00841873_m1), differentiated macrophages (CD68, Mm00839636_g1; Mac3, Mn00495267_m1), TNF-α (Mm00443258-m1), MPO (Mm00447886_m1), TGF-β (Mm00436971_m1), and appropriate controls (GAPDH, apoE).

Imaging

To evaluate the prognostic significance of ex vivo findings, we assessed monocyte-associated biomarkers in the infarct and followed in parallel left ventricular remodeling in the same cohort of mice. This approach used FMT-CT as a molecular imaging tool and MRI to quantitate physiological variables, a powerful and effective combination to follow the events post MI longitudinally.

FMT-CT—To validate the FMT-CT fusion algorithm, we used a tissue phantom filled with a solution of 30 μl CT contrast (Isovue-370, Bracco) and 1 nmol of the fluorochrome VT-680 (VisEn Medical). Using a FMT 2500 system (VisEn Medical), we acquired 30 frontal slices of 0.5 mm thickness in z-direction, with an in-plane resolution of 1×1 mm. Data were post-processed using a normalized Born forward equation to calculate three-dimensional fluorochrome concentration maps. The phantom was then imaged by CT while positioned in a multimodality cartridge.

On day 5 after MI, one day after onset of the monocytic Phase 2,16 we performed dual channel (680/700 nm and 750/800 nm excitation/emission) FMT-CT imaging to interrogate the magnitude and quality of inflammation 24 hours after injection of 5 nmol of a pan-cathepsin protease sensor (Prosense-680) and 15 mg/kg body weight CLIO-750, nanoparticles prone to be ingested by phagocytes.[21] A 3D dataset was reconstructed in which fluorescence per voxel was expressed in nM. To robustly identify the region of interest in the heart, anatomic imaging with CT immediately followed FMT. The imaging cartridge containing the anesthetized mouse was placed into the custom machined Plexiglas holder that supplies isoflurane, warm air and optimal positioning in the CT (Inveon PET-CT, Siemens). The CT x-ray source operated at 80 kVp and 500 μA with an exposure time of 370 - 400 ms. The effective 3D resolution was 80 μm isotropic. Isovue-370 was infused intravenously at 55 μL/min through a tail vein catheter. The CT reconstruction protocol performed bilinear interpolation, used a Shepp-Logan filter, and scaled pixels to Hounsfield units.

Image fusion—The fusion method realized three-dimensional mapping of fluorescence within the anatomical reference CT. The approach was based on a multimodality-compatible animal holding device that provides fiducial landmarks on its frame. The imaging cartridge lightly compressed the anesthetized mouse between optically translucent windows and thereby prevented motion during transfer between modalities. The three-dimensional distribution of the fiducials enabled co-registration of datasets in an automated fashion. The point based coregistration tool kit in OsiriX shareware fused images after identification of fiducials in respective modalities. Fiducials were tagged with point markers to define their XYZ coordinates. Using these coordinates, data were resampled, rotated and translated to match the image matrices, and finally fused.

MRI—We performed in vivo MRI on day 1 and day 21 after MI in the same mice that were imaged by FMT-CT to follow the functional impact of infarct healing on the evolution of heart failure. A 7 Tesla horizontal bore Pharmascan (Bruker) was used to obtain hyperenhancement cine images of the left ventricular short axis after injection of Gd-DTPA (Berlex) at a dosage of 0.3 mmol/kg.[22] We employed ECG and respiratory gating using a T1 weighted gradient echo sequence (echo time 2.7 ms, 16 frames per RR interval); flip angle 60 degrees; in-plane resolution 200×200 μm; slice thickness 1 mm). Cardiac volumes were quantitated from 6-8 short axis imaging slices covering the left ventricle. The infarcted area was identified in end-diastolic frames as a) hypokinetic in cine loops and b) hyperenhancing after Gd-DTPA injection. Changes of parameters over time were then calculated, i.e. $\Delta EDV = EDV_{day21} - EDV_{day1}$.

Statistics

Results are expressed as mean ± SEM. Statistical comparisons between two groups were evaluated by Student's t-test. $P < 0.05$ was considered to indicate statistical significance.

Results

We first investigated if elevated blood levels of inflammatory Ly-6C^{hi} monocytes in atherosclerotic apoE$^{-/-}$ mice (reference[12] and corroborated in the present study, Fig. 2) result in increased and prolonged presence of these cells in the healing infarct. We collected infarcts on day 5 because this time point represents the start of Phase 2, i.e., the healing phase dominated by anti-inflammatory Ly-6C^{lo} monocytes in wild type mice.[16] While the number of Ly-6C^{hi} monocytes in wild type mice had already declined ($1.1\pm0.1 \times 10^4$ cells in heart), we found >10-times more Ly-6C^{hi} cells in infarcts of apoE$^{-/-}$ mice ($14.4\pm5.8 \times 10^4$ cells, $p<0.05$, Fig. 2). The ratio of Ly-6C^{hi} to Ly-6C^{lo} in infarct tissue was 1.2 for wild type and 2.2 for apoE$^{-/-}$ mice. ApoE$^{-/-}$ mice also showed higher numbers of neutrophils and macrophages (Fig. 2); the latter likely derive from Ly-6C^{hi} monocytes.[12]

Monocyte subsets exhibit functional heterogeneity, and Ly-6C^{hi} monocytes selectively show higher inflammatory activity.[23] Thus, we investigated the inflammatory status of infarct tissue by immunohistochemistry and gene expression analysis. Quantitative staining showed increased cathepsin B (target enzyme of the fluorescent protease imaging sensor), MMP2 and MMP9 enzymes in infarcts of apoE$^{-/-}$ compared to wild type mice (Fig. 3A). The number of CD31^{+} microvessels was higher in apoE$^{-/-}$ mice, likely due to higher inflammatory cell numbers that shuttle in proteases and VEGF (Fig. 3A). Interestingly, MMP9 has been reported to promote VEGF release in cancer.[24] mRNA levels of the inflammatory enzyme myeloperoxidase (MPO) and TNF-α increased in apoE$^{-/-}$ infarct tissue, whereas mRNA levels of TGF-β, a protein that stimulates fibroblast function and collagen deposition to strengthen the evolving infarct scar,[1-4] declined (Fig. 3B). qPCR confirmed increased levels of Ly-6C (monocytes), and CD68 and MAC-3 (macrophages, Fig. 3B). We also compared monocyte subsets directly for proteolysis and phagocytosis. This involved i.v. injection of an activatable pan-cathepsin sensor (Prosense-680) and a phagocytosis sensor (CLIO-750), followed by flow cytometry analysis of cell suspensions isolated from infarcts. Ly-6C^{hi} monocytes showed 7.5-times more protease activity than their Ly-6C^{lo} counterparts in vivo, whereas both subsets had similar phagocytic activity (Table 1). Both activities were lower in CD11b^{-} cells (mostly T and B cells) and neutrophils (Table 1). These data indicate that the prolonged Phase I Ly-6C^{hi} monocyte response in infarcts of apoE$^{-/-}$ mice associates with heightened inflammatory activity.

The results above indicate that the activatable pan-cathepsin sensor should report selectively on Ly-6C^{hi} monocytes in vivo, while the phagocytosis sensor indicates the presence of both monocyte subsets. Thus, we thought to use these agents in combination with fusion FMT-CT imaging to map the monocyte response in infarct tissues in vivo (FMT detects molecular signal, whereas CT gives anatomical information). Initially, we performed phantom validation experiments to evaluate the accuracy of fusion of datasets obtained from the two imaging modalities. Phantoms placed in a multimodality mouse holder (Fig. 4A) underwent imaging with both modalities. Fusion was performed using fiducial landmarks on the holder frame (Fig. 4B-D). We then measured the distance between the phantom cavity, which was filled with a CT contrast/fluorochrome solution, and the edge of the phantom on CT images (Fig. 4B). The same measurement was repeated on the fused FMT-CT data set but here the cavity was identified using the fluorescence signal. We observed excellent spatial co-registration and correlation ($R^2=0.994$, $p<0.001$, Fig. 4D, E). Next, we evaluated a wild type mouse post coronary ligation injected with CLIO-750 to report on phagocytic activity. CT allowed to assess anatomy while FMT-CT fusion showed the fluorescence signal localized in the left side of the thoracic cavity, a finding that was consistent with uptake into the infarct region (Fig. 4F-K). We then investigated in vivo cathepsin and phagocytic activities in infarcts of apoE$^{-/-}$ mice during monocytic healing Phase 2, when the protease activity has passed its peak[21] and the number of Ly-6C^{hi} monocytes has declined in infarcts of wild type

mice.[16] As outlined in the serial imaging protocol (Fig. 1), we first assessed infarct size by delayed enhancement MRI, which showed no significant difference between groups (wild type 16 ± 3%, apoE$^{-/-}$ 14 ± 2%, p = 0.6). In some apoE$^{-/-}$ mice, CT showed vascular calcification in the aortic wall coincident with atherosclerotic plaques. Two- and three-dimensional reconstructions of fused FMT-CT images showed Prosense-680 and CLIO-750 signals in the apex of the left ventricle. Corresponding to the increase of Ly-6C^{hi} monocytes and macrophages by flow cytometry, histology and PCR data, we found higher protease and phagocytic activity in infarcts of apoE$^{-/-}$ mice ($p<0.05$, Fig. 5A). Ex vivo reflectance fluorescence imaging of myocardial rings harvested from a separate group of mice corroborated our in vivo FMT findings. The target to background ratio for both molecular probes was higher in the infarct of apoE$^{-/-}$ mice when compared to wild type mice ($p<0.0001$, Fig. 5B). Ex vivo, Prosense-680 signal was 2.7-fold and CLIO-750 signal 3.3-fold higher in apoE$^{-/-}$ infarcts when compared to wild type mice, alike to the differences seen in vivo (FMT for Prosense-680 and CLIO-750: 2.9-fold and 2.6-fold increase in apoE$^{-/-}$ mice, respectively). Of note, the fluorescence of infarcts in wild type mice, although lower than that in apoE$^{-/-}$ animals, exceeded significantly the signals in sham-operated controls that received the molecular sensors without coronary artery ligation ($p<0.0001$).

We next quantitated left ventricular remodeling with serial cine MRI. We observed similar myocardial hypertrophy in wild type and apoE$^{-/-}$ mice (Fig. 6). While EF was comparable between groups on day 1 after MI, enhanced ventricular dilation of the LV tripled its decline between day 1 and day 21 in apoE$^{-/-}$ mice. MRI-derived increase in end-diastolic volume positively correlated with protease activity measured with FMT (Prosense-680 activation, $R^2=0.39$, $p=0.003$), but not with phagocytic activity (CLIO-750 uptake, $p=0.24$). The correlation of FMT-derived protease signal with left ventricular dilation implies that i) protease sensing can predict post-MI heart failure and ii) prolonged retention of proteolytic Ly-6C^{hi} monocytes impairs infarct healing and ventricular remodeling.

Phenotypic changes in apoE$^{-/-}$ mice with high-cholesterol diet may not be limited to the change in monocyte subsets. Thus, we thought to investigate whether Ly-6C^{hi} monocytosis is causally linked to LV remodeling. To this end, we investigated an independent mouse model in which monocytosis is not related to germline deletion of apoE and hyperlipidemia, but is induced experimentally in wild-type mice by repeated injections of LPS.[20] Flow cytometry on day 5 after MI showed increased numbers of monocytes in blood and in infarcts, comparable to our observations in apoE$^{-/-}$ mice (Fig. 7A). FMT-CT showed increased protease and phagocytic signal, and MRI showed increased ventricular dilation in LPS-treated mice in vivo (Fig. 7A). Thus, increased inflammation in infarct tissue and subsequent heart failure are both recapitulated in wild-type mice with artificially–induced monocytosis. Of note, the LPS treatment did not alter the recruitment of neutrophils, which represent another important cellular mediator of inflammation after MI (Fig 7A). Also, in vivo depletion of neutrophils in apoE$^{-/-}$ mice did not restore post MI remodeling (Fig 7B). These data indicate that the number of Ly-6C^{hi} monocytes recruited into the infarct has direct consequences on LV remodeling.

Discussion

Monocyte/macrophages contribute centrally to wound healing. Their known functions include removal of necrotic debris, propagation of angiogenesis, and regulation of extracellular matrix turnover.[23, 25] These phagocytes elaborate regulatory cytokines, chemokines and proteolytic enzymes, all of which participate in tissue repair.[1-4] Experimental[16, 26] and clinical data[27] show that abrogation of monocytes compromises infarct healing. However, little is known about the down-regulation of innate immune cell activity and associated inflammation after the initial burst triggered by ischemic myocardial

injury. Here we show that effective infarct healing necessitates timely and coordinated resolution of inflammation. The endogenous repair response that follows MI requires immune cell populations which are profoundly altered during atherosclerosis, the condition that causes MI in most patients. Specifically, we found that Ly-6C^{hi} monocytes, which are chronically expanded in the blood pool of atherosclerotic apoE$^{-/-}$ mice, impair infarct healing through prolonged presence in the infarct, delayed onset of monocytic phase 2 and deregulated resolution of inflammation.

The increased circulating pool of Ly-6C^{hi} monocytes in apoE$^{-/-}$ mice corresponded to a higher number of this inflammatory subset lingering in the infarct 5 days after MI, presumably because an excess of these cells in the circulation leads to their more abundant recruitment. The gene expression profile of apoE$^{-/-}$ infarcts remained pro-inflammatory when inflammation was already waning in wild type infarcts. For instance, myeloperoxidase activity peaks 2 days after MI in wild type mice and quickly resolves thereafter.[28] In the current study, we found that MPO transcription was still >3-fold higher in apoE$^{-/-}$ infarcts on day 5. Therefore, we speculate that the increased residual Ly-6C^{hi} monocytes in the myocardial infarcts of apoE$^{-/-}$ mice hampered transition towards an anti-inflammatory healing microenvironment. Future studies will need to determine the precise mechanisms responsible for elevated Ly-6C^{hi} monocyte presence in the myocardium of these mice. Notably, hypercholesterolemia has been shown to promote monocyte proliferation and survival[12] and may therefore modulate Phase I to Phase II transition. However, LPS-induced monocytosis also resulted in sustained infarct inflammation and accelerated ventricular dilation, suggesting that blood monocytosis may hamper resolution of inflammation in the infarct. Furthermore, although neutrophil depletion did not improve remodeling in apoE$^{-/-}$ mice, the role of the prolonged presence of these cells requires further study.

The use of non-invasive molecular and physiological imaging[29] allowed us to correlate the inflammatory milieu in the infarct[30] in vivo with the development of heart failure. Infarcts of apoE$^{-/-}$ mice had higher protease activity and increased phagocytic rates compared to those in wild type mice. Flow cytometric probe distribution studies suggested that this constellation is caused by a high number of Ly-6C^{hi} monocytes in apoE$^{-/-}$ infarcts, since the inflammatory subset activates more protease sensor moieties per monocyte. Consequently, ventricular dilation was accelerated and resulted in a 16% lower ejection fraction 3 weeks after MI in apoE$^{-/-}$ mice. Cathepsin activity, by virtue of its association with Ly-6C^{hi} monocytes, is an integral component of the early monocytic phase of myocardial repair. The positive correlation between enzyme activity and left ventricular dilation suggests that a prolonged Phase I or a compromised Phase II predisposes to heart failure. Translation of this diagnostic concept might permit identification of infarct patients at accentuated risk for developing heart failure.

The results of our study point to inflammatory monocytes as a potential therapeutic target in post MI heart failure, whose modulation might augment healing and attenuate left ventricular remodeling. Future work should search for measures to support the Ly-6C^{hi}→ Ly-6C^{lo} subset recruitment switch and to chaperone the healing microenvironment towards dampened inflammation during the second monocytic phase. Molecular imaging that interrogates monocytic targets in injured myocardium in conjunction with quantitation of monocyte subsets in the circulation might provide prognostic information and help guide therapies to promote favorable ventricular remodeling post myocardial infarction.

Acknowledgments

The authors acknowledge help from members of the Mouse Imaging Program (MIP); Anne Yu, BS; Alexandra Kunin, BS; Elisabeth Zhang, BS; Brett Marinelli, BS; for help with imaging and data processing, Yoshiko

Iwamoto, BS for histological staining, Nikolai Sergeyev, PhD for nanoparticle synthesis. Wael Yared, PhD, and Thorsten Mempel, PhD, are acknowledged for helpful discussions.

Funding Sources: This work was funded in part by NIH grants to Ralph Weissleder (UO1-HL-080731, RO1-EB006432, T32-CA79443, R24-CA92782, P50-CA86355), and Matthias Nahrendorf (R01HL096576-01) and an American Heart Association grant (0835623D) to Matthias Nahrendorf.

References

1. Frangogiannis NG, Entman ML. Targeting the chemokines in myocardial inflammation. Circulation 2004;110(11):1341–1342. [PubMed: 15364818]
2. Blankesteijn WM, Creemers E, Lutgens E, Cleutjens JP, Daemen MJ, Smits JF. Dynamics of cardiac wound healing following myocardial infarction: observations in genetically altered mice. Acta Physiol Scand 2001;173(1):75–82. [PubMed: 11678729]
3. Cleutjens JP, Blankesteijn WM, Daemen MJ, Smits JF. The infarcted myocardium: simply dead tissue, or a lively target for therapeutic interventions. Cardiovasc Res 1999;44(2):232–241. [PubMed: 10690298]
4. Ertl G, Frantz S. Healing after myocardial infarction. Cardiovasc Res 2005;66(1):22–32. [PubMed: 15769445]
5. Sutton MG, Sharpe N. Left ventricular remodeling after myocardial infarction: pathophysiology and therapy. Circulation 2000;101(25):2981–2988. [PubMed: 10869273]
6. Lee KL, Woodlief LH, Topol EJ, Weaver WD, Betriu A, Col J, Simoons M, Aylward P, Van de Werf F, Califf RM. Predictors of 30-day mortality in the era of reperfusion for acute myocardial infarction. Results from an international trial of 41,021 patients. GUSTO-I Investigators. Circulation 1995;91(6):1659–1668. [PubMed: 7882472]
7. Dargie HJ. Effect of carvedilol on outcome after myocardial infarction in patients with left-ventricular dysfunction: the CAPRICORN randomised trial. Lancet 2001;357(9266):1385–1390. [PubMed: 11356434]
8. Latini R, Tognoni G, Maggioni AP, Baigent C, Braunwald E, Chen ZM, Collins R, Flather M, Franzosi MG, Kjekshus J, Kober L, Liu LS, Peto R, Pfeffer M, Pizzetti F, Santoro E, Sleight P, Swedberg K, Tavazzi L, Wang W, Yusuf S. Clinical effects of early angiotensin-converting enzyme inhibitor treatment for acute myocardial infarction are similar in the presence and absence of aspirin: systematic overview of individual data from 96,712 randomized patients. Angiotensin-converting Enzyme Inhibitor Myocardial Infarction Collaborative Group. J Am Coll Cardiol 2000;35(7):1801–1807. [PubMed: 10841227]
9. Pfeffer MA, Braunwald E, Moye LA, Basta L, Brown EJ Jr, Cuddy TE, Davis BR, Geltman EM, Goldman S, Flaker GC, et al. Effect of captopril on mortality and morbidity in patients with left ventricular dysfunction after myocardial infarction. Results of the survival and ventricular enlargement trial. The SAVE Investigators. The New England Journal of Medicine 1992;327(10): 669–677. [PubMed: 1386652]
10. AHA. Cardiovascular Disease Statistics. 2008. www.americanheart.org
11. Libby P. Inflammation in atherosclerosis. Nature 2002;420(6917):868–874. [PubMed: 12490960]
12. Swirski FK, Libby P, Aikawa E, Alcaide P, Luscinskas FW, Weissleder R, Pittet MJ. Ly-6Chi monocytes dominate hypercholesterolemia-associated monocytosis and give rise to macrophages in atheromata. J Clin Invest 2007;117(1):195–205. [PubMed: 17200719]
13. Tacke F, Alvarez D, Kaplan TJ, Jakubzick C, Spanbroek R, Llodra J, Garin A, Liu J, Mack M, van Rooijen N, Lira SA, Habenicht AJ, Randolph GJ. Monocyte subsets differentially employ CCR2, CCR5, and CX3CR1 to accumulate within atherosclerotic plaques. J Clin Invest 2007;117(1):185–194. [PubMed: 17200718]
14. Schlitt A, Heine GH, Blankenberg S, Espinola-Klein C, Dopheide JF, Bickel C, Lackner KJ, Iz M, Meyer J, Darius H, Rupprecht HJ. CD14+CD16+ monocytes in coronary artery disease and their relationship to serum TNF-alpha levels. Thrombosis and Haemostasis 2004;92(2):419–424. [PubMed: 15269840]

15. Heine GH, Ulrich C, Seibert E, Seiler S, Marell J, Reichart B, Krause M, Schlitt A, Kohler H, Girndt M. CD14(++)CD16+ monocytes but not total monocyte numbers predict cardiovascular events in dialysis patients. Kidney International 2008;73(5):622–629. [PubMed: 18160960]

16. Nahrendorf M, Swirski FK, Aikawa E, Stangenberg L, Wurdinger T, Figueiredo JL, Libby P, Weissleder R, Pittet MJ. The healing myocardium sequentially mobilizes two monocyte subsets with divergent and complementary functions. The Journal of Experimental Medicine 2007;204(12):3037–3047. [PubMed: 18025128]

17. Maekawa Y, Anzai T, Yoshikawa T, Asakura Y, Takahashi T, Ishikawa S, Mitamura H, Ogawa S. Prognostic significance of peripheral monocytosis after reperfused acute myocardial infarction:a possible role for left ventricular remodeling. J Am Coll Cardiol 2002;39(2):241–246. [PubMed: 11788214]

18. Mariani M, Fetiveau R, Rossetti E, Poli A, Poletti F, Vandoni P, D'Urbano M, Cafiero F, Mariani G, Klersy C, De Servi S. Significance of total and differential leucocyte count in patients with acute myocardial infarction treated with primary coronary angioplasty. European Heart Journal 2006;27(21):2511–2515. [PubMed: 16923741]

19. Nahrendorf M, Hu K, Frantz S, Jaffer FA, Tung CH, Hiller KH, Voll S, Nordbeck P, Sosnovik D, Gattenlohner S, Novikov M, Dickneite G, Reed GL, Jakob P, Rosenzweig A, Bauer WR, Weissleder R, Ertl G. Factor XIII deficiency causes cardiac rupture, impairs wound healing, and aggravates cardiac remodeling in mice with myocardial infarction. Circulation 2006;113(9):1196–1202. [PubMed: 16505171]

20. O'Connell RM, Rao DS, Chaudhuri AA, Boldin MP, Taganov KD, Nicoll J, Paquette RL, Baltimore D. Sustained expression of microRNA-155 in hematopoietic stem cells causes a myeloproliferative disorder. The Journal of Experimental Medicine 2008;205(3):585–594. [PubMed: 18299402]

21. Nahrendorf M, Sosnovik DE, Waterman P, Swirski FK, Pande AN, Aikawa E, Figueiredo JL, Pittet MJ, Weissleder R. Dual channel optical tomographic imaging of leukocyte recruitment and protease activity in the healing myocardial infarct. Circ Res 2007;100(8):1218–1225. [PubMed: 17379832]

22. Yang Z, Berr SS, Gilson WD, Toufektsian MC, French BA. Simultaneous evaluation of infarct size and cardiac function in intact mice by contrast-enhanced cardiac magnetic resonance imaging reveals contractile dysfunction in noninfarcted regions early after myocardial infarction. Circulation 2004;109(9):1161–1167. [PubMed: 14967719]

23. Gordon S, Taylor PR. Monocyte and macrophage heterogeneity. Nat Rev Immunol 2005;5(12):953–964. [PubMed: 16322748]

24. Bergers G, Brekken R, McMahon G, Vu TH, Itoh T, Tamaki K, Tanzawa K, Thorpe P, Itohara S, Werb Z, Hanahan D. Matrix metalloproteinase-9 triggers the angiogenic switch during carcinogenesis. Nature Cell Biology 2000;2(10):737–744.

25. Singer AJ, Clark RA. Cutaneous wound healing. The New England Journal of Medicine 1999;341(10):738–746. [PubMed: 10471461]

26. van Amerongen MJ, Harmsen MC, van Rooijen N, Petersen AH, van Luyn MJ. Macrophage depletion impairs wound healing and increases left ventricular remodeling after myocardial injury in mice. Am J Pathol 2007;170(3):818–829. [PubMed: 17322368]

27. Roberts R, DeMello V, Sobel BE. Deleterious effects of methylprednisolone in patients with myocardial infarction. Circulation 1976;53(3 Suppl):I204–206. [PubMed: 1253361]

28. Nahrendorf M, Sosnovik D, Chen JW, Panizzi P, Figueiredo JL, Aikawa E, Libby P, Swirski FK, Weissleder R. Activatable Magnetic Resonance Imaging Agent Reports Myeloperoxidase Activity in Healing Infarcts and Noninvasively Detects the Antiinflammatory Effects of Atorvastatin on Ischemia-Reperfusion Injury. Circulation. 2008

29. Sanz J, Fayad ZA. Imaging of atherosclerotic cardiovascular disease. Nature 2008;451(7181):953–957. [PubMed: 18288186]

30. Su H, Spinale FG, Dobrucki LW, Song J, Hua J, Sweterlitsch S, Dione DP, Cavaliere P, Chow C, Bourke BN, Hu XY, Azure M, Yalamanchili P, Liu R, Cheesman EH, Robinson S, Edwards DS, Sinusas AJ. Noninvasive targeted imaging of matrix metalloproteinase activation in a murine model of postinfarction remodeling. Circulation 2005;112(20):3157–3167. [PubMed: 16275862]

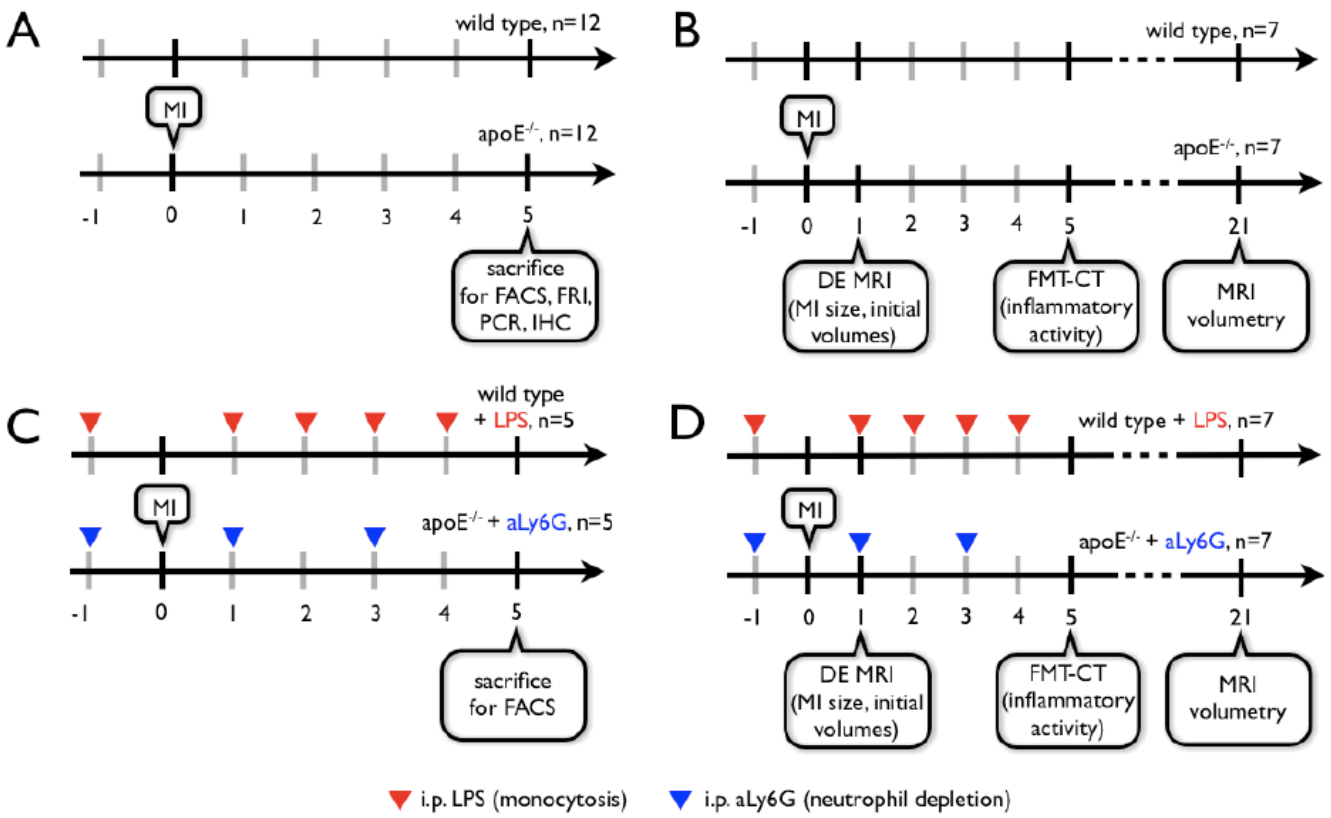

Figure 1.

Experimental protocol for ex (A, C) and in vivo (B, D) studies. MI: myocardial infarction induced by coronary ligation, FRI: ex vivo Fluorescence Reflectance Imaging, FACS: Fluorescence Activated Cell Sorting, PCR: Polymerase Chain Reaction-based gen expression profiling, IHC: Immunohistochemistry, DE MRI: delayed enhancement MRI for infarct size measurement.

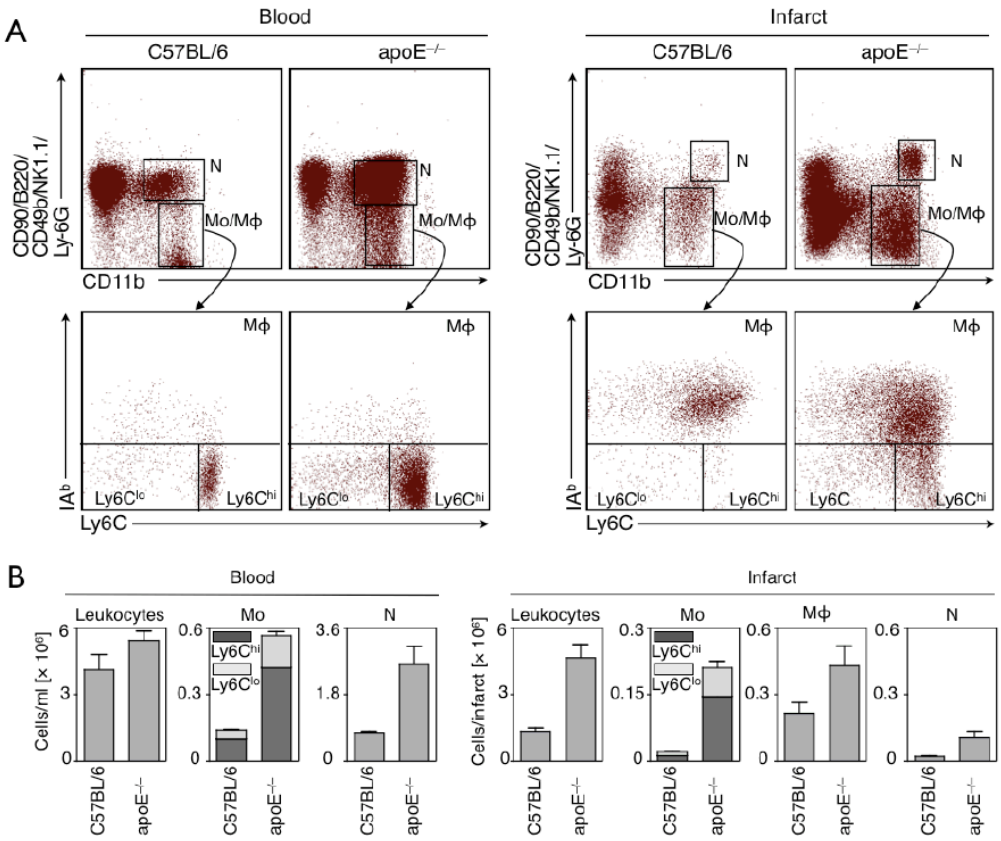

Figure 2.

(A) Original flow cytometry dot plots of blood and infarct tissue in wild type and apoE$^{-/-}$ mice 5 days after coronary ligation. (B) Enumeration of cells shows significantly increased blood and tissue levels for inflammatory Ly-6C^{hi} monocytes in apoE$^{-/-}$ mice.

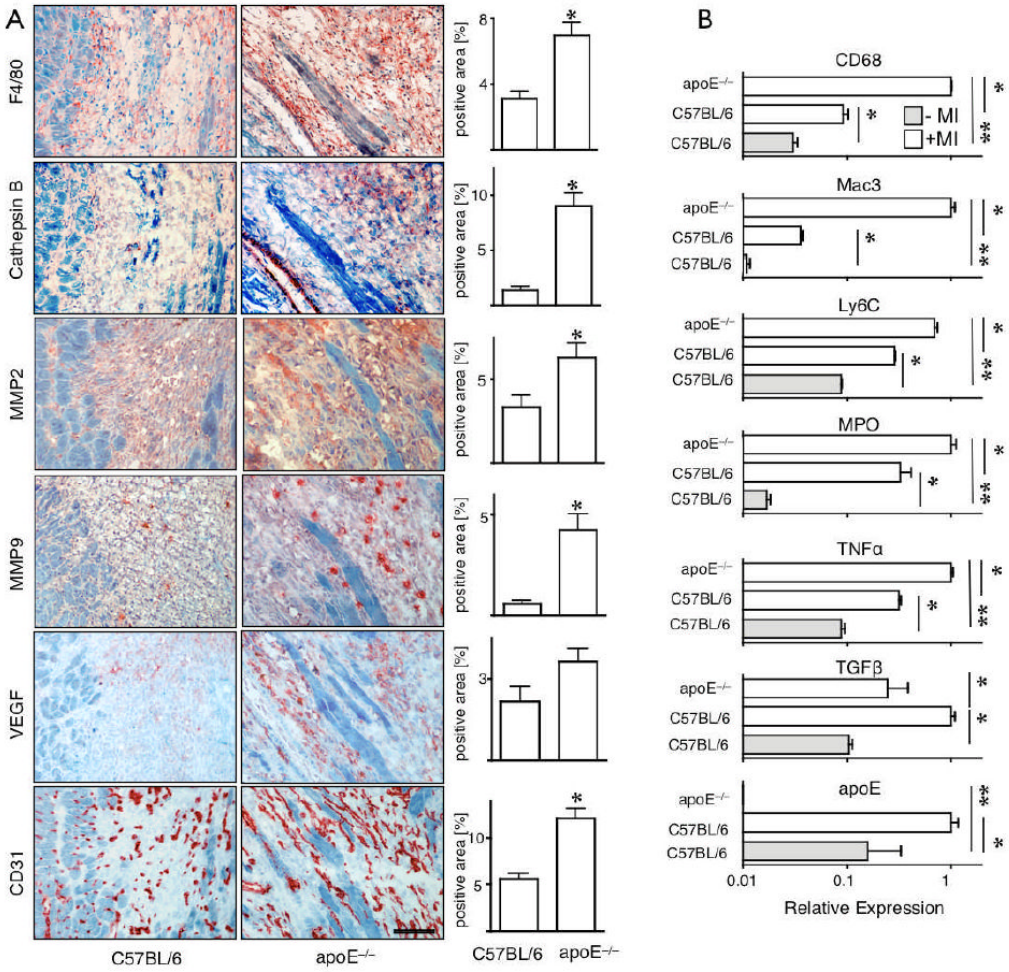

Figure 3.

(A) Immunoreactive staining and quantitation for the presence of the imaging target protease Cathepsin B and F4/80 positive macrophages. Furthermore, presence of MMP2, MMP9, VEGF and CD31 was profiled. Magnification 200×, the scale bar denotes 100 μm. (B) Quantitative RT-PCR: higher expression of MAC-3 and CD68 corroborate in vivo and ex vivo findings of increased cell recruitment into the infarct of apoE$^{-/-}$. Transcription of MPO and TNF-α is higher in apoE$^{-/-}$ mice, whereas TGF-β is reduced. As a control, we determined apoE, which was undetectable in apoE$^{-/-}$ mice. *p<0.05, **p<0.001.

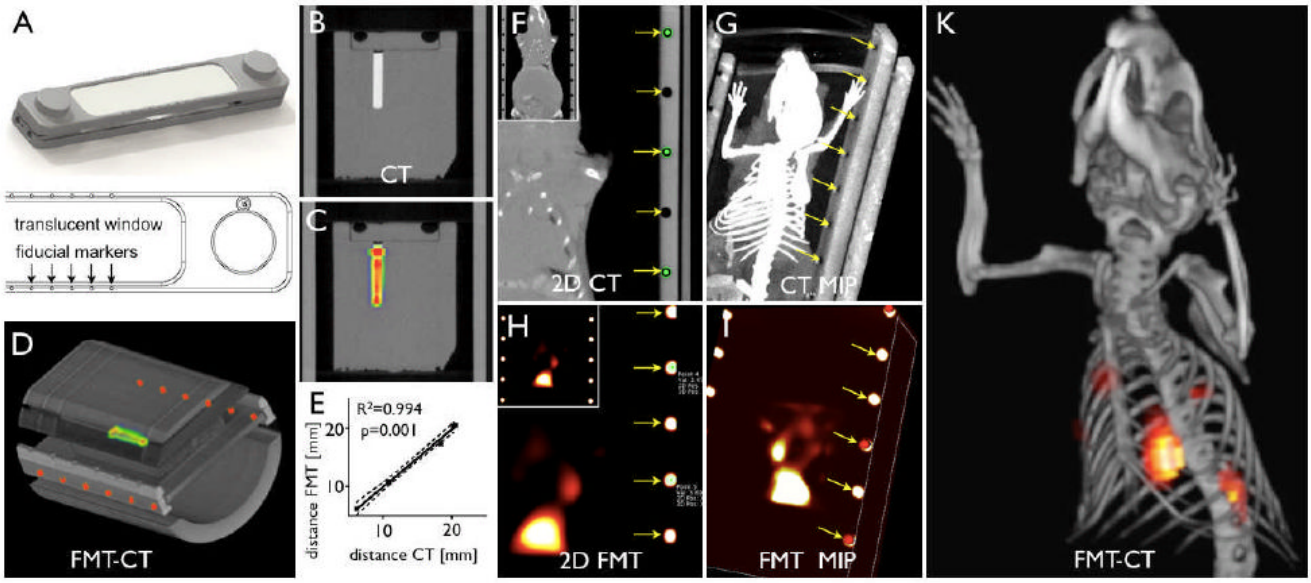

Figure 4.

Image fusion. (A) Multimodal imaging cartridge. (B-E) FMT-CT phantom imaging. (B-C) Coronal CT and FMT-CT. (D) Maximum intensity projection of fused FMT-CT. The well inside the phantom is filled with fluorochrome VT-680 and in addition contains iodine CT contrast. (E) Correlation between CT and FMT-CT dimensions shows good agreement of fused data. (F-K) CT, FMT and FMT-CT in a mouse with MI injected with CLIO. Arrows denote fiducial landmarks used for fusion.

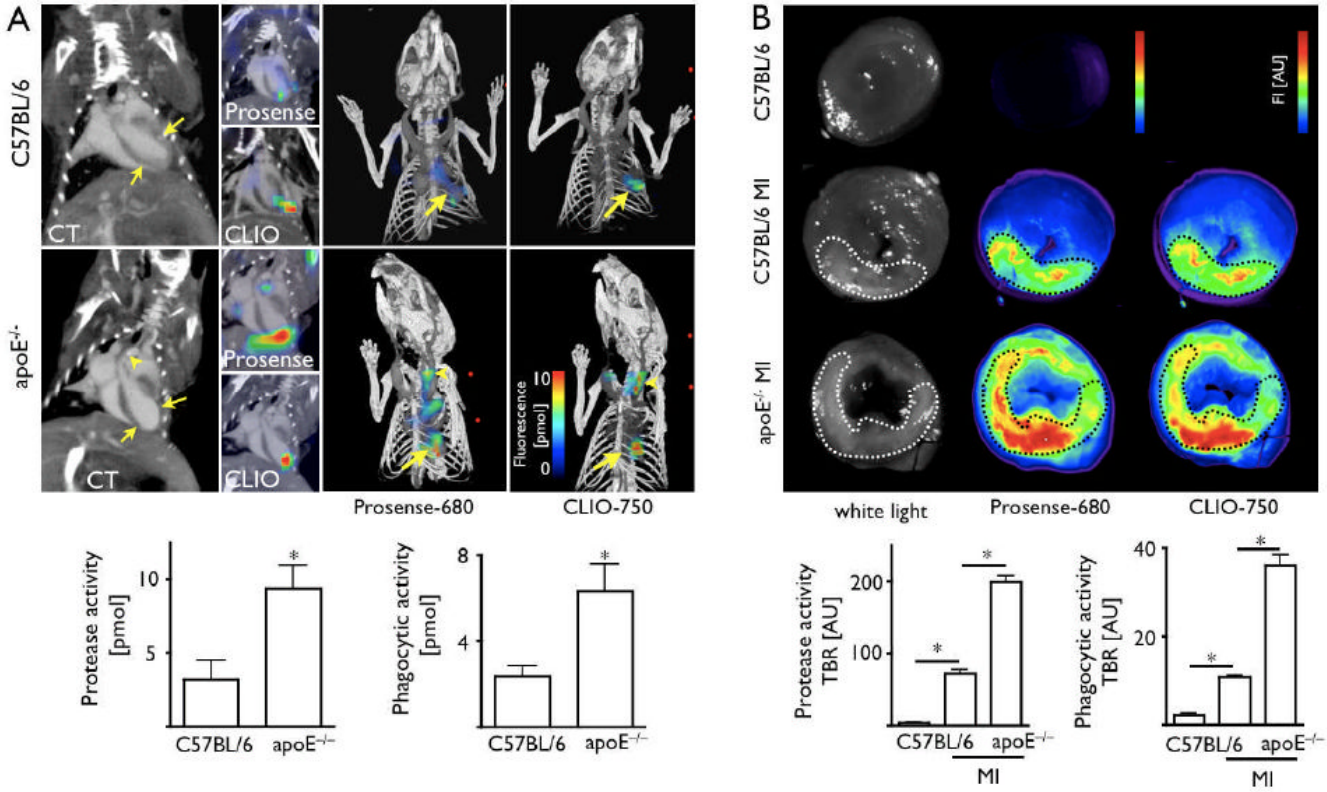

Figure 5.

(A) FMT-CT 5 days after MI. Arrows denote apical infarct, arrowhead denotes calcification, presumably in an atherosclerotic lesion. On 3D Prosense and CLIO FMT-CT images, arrows point towards infarct signal. Arrowheads denote fluorescence signal in the carotid artery. (B) Ex vivo fluorescence reflectance imaging corroborates in vivo FMT findings. TBR: target to background ratio. *$p<0.05$.

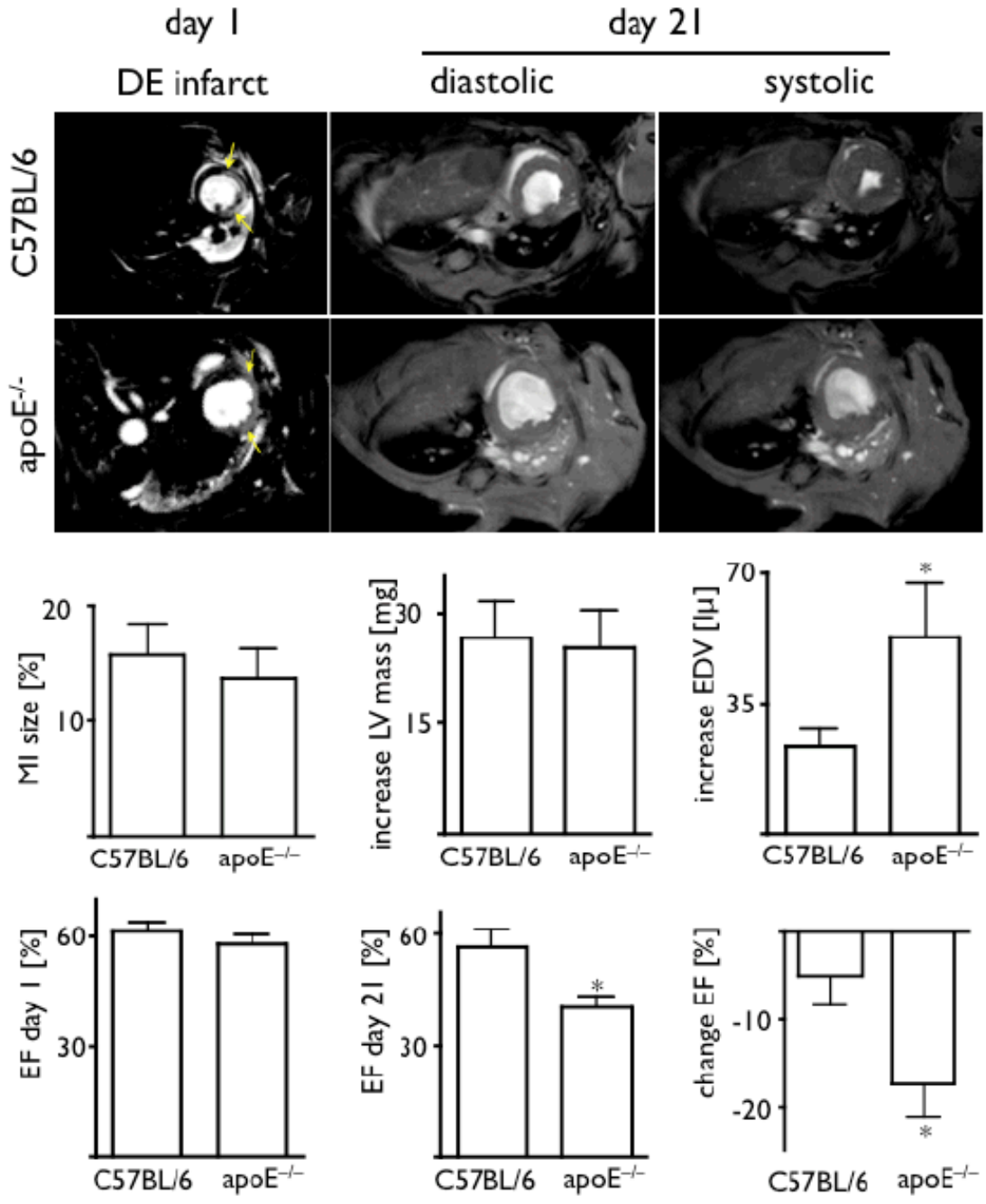

Figure 6.

Serial cardiac MRI. Initial assessment of infarct size by delayed enhancement after injection of Gd-DTPA (arrows) showed similar values in both groups. Over time, ventricular dilatation was enhanced in apoE$^{-/-}$ mice, which resulted in significantly worse EF on day 21 after MI. *p<0.05.

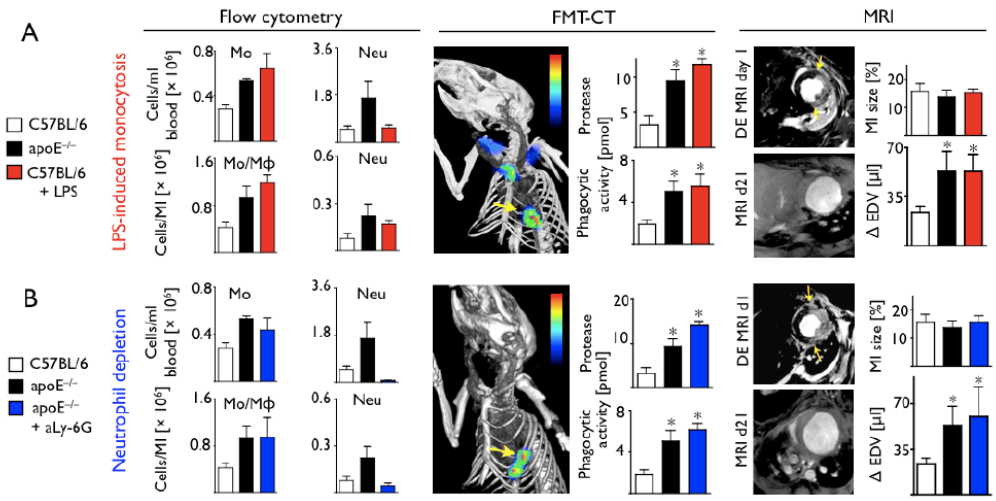

Figure 7.

(A) Flow cytometry on day 5 and serial imaging in wild type mice in which blood monocytosis was induced by LPS. Blood monocytosis led to sustained monocyte presence in the infarct on day 5, increased protease and phagocytic signal on FMT and accelerated left ventricular dilation. (B) ApoE$^{-/-}$ mice in which neutrophils were depleted with injections of anti-Ly-6G antibody show similar inflammation in the infarct by FMT-CT and remodeling by MRI. *p<0.05.

Table 1
Per cell fluorescence 24hrs after IV injection

Mean fluorescence intensity per cell after injection of respective sensor measured by flow cytometry. Cells were retrieved from infarcts. Protease signal (Prosense) is highest Ly-6C^{hi} monocytes.

Cell	Prosense	CLIO
Ly-6C^{hi} monocyte	8902 ± 2747	1191 ± 6
Ly-6C^{lo} monocyte	1433 ± 343	1125 ± 41
neutrophil	1930 ± 200	340 ± 56
lymphocyte	525 ± 103	214 ± 51

Table 2

Heart and body weights

Heart and body weights 3 weeks after MI.

	heart weight [mg]	body weight [g]
C57/BL6	167.9±4.0	22.3±1.5
apoE$^{-/-}$	171.5±9.4	23.0±0.8